# R-Spondin1 expands Paneth cells and prevents dysbiosis induced by graft-versus-host disease

Eiko Hayase,[1] Daigo Hashimoto,[1] Kiminori Nakamura,[2] Clara Noizat,[1] Reiki Ogasawara,[1] Shuichiro Takahashi,[1] Hiroyuki Ohigashi,[1] Yuki Yokoi,[3] Rina Sugimoto,[3] Satomi Matsuoka,[1] Takahide Ara,[1] Emi Yokoyama,[1] Tomohiro Yamakawa,[1] Ko Ebata,[1] Takeshi Kondo,[1] Rina Hiramine,[4,5] Tomoyasu Aizawa,[4,5] Yoshitoshi Ogura,[6] Tetsuya Hayashi,[6] Hiroshi Mori,[7] Ken Kurokawa,[7,8] Kazuma Tomizuka,[9] Tokiyoshi Ayabe,[2] and Takanori Teshima[1]

[1]Department of Hematology, Faculty of Medicine, Graduate School of Medicine, [2]Department of Cell Biological Science, Graduate School of Life Science, Faculty of Advanced Life Science, [3]Innate Immunity Laboratory, Graduate School of Life Science, [4]Department of Protein Science Laboratory, Graduate School of Life Science, and [5]Global Station for Soft Matter, Global Institution for Collaborative Research and Education, Hokkaido University, Sapporo, Japan
[6]Department of Bacteriology, Faculty of Medical Sciences, Kyushu University, Fukuoka, Japan
[7]Center for Information Biology, National Institute of Genetics, Mishima, Japan
[8]Department of Life Science and Technology, Tokyo Institute of Technology, Tokyo, Japan
[9]Innovative Technology Labs, Research Functions Unit, Research & Development Division, Kyowa Hakko Kirin, Tokyo, Japan

**The intestinal microbial ecosystem is actively regulated by Paneth cell–derived antimicrobial peptides such as α-defensins. Various disorders, including graft-versus-host disease (GVHD), disrupt Paneth cell functions, resulting in unfavorably altered intestinal microbiota (dysbiosis), which further accelerates the underlying diseases. Current strategies to restore the gut ecosystem are bacteriotherapy such as fecal microbiota transplantation and probiotics, and no physiological approach has been developed so far. In this study, we demonstrate a novel approach to restore gut microbial ecology by Wnt agonist R-Spondin1 (R-Spo1) or recombinant α-defensin in mice. R-Spo1 stimulates intestinal stem cells to differentiate to Paneth cells and enhances luminal secretion of α-defensins. Administration of R-Spo1 or recombinant α-defensin prevents GVHD-mediated dysbiosis, thus representing a novel and physiological approach at modifying the gut ecosystem to restore intestinal homeostasis and host–microbiota cross talk toward therapeutic benefits.**

## INTRODUCTION

Trillions of microbes inhabit mammals, with the largest population in the intestinal tract, and play vital roles in a host's metabolism and immunity (Qin et al., 2010). Composition of intestinal microbiota is mainly maintained by luminal secretion of antimicrobial peptides (AMPs) from Paneth cells. α-Defensins are the most bactericidal AMPs released from Paneth cells (Ayabe et al., 2000; Salzman et al., 2010). Emerging evidence demonstrates that Paneth cell functions are impaired in various inflammatory and metabolic disorders, resulting in unfavorably altered intestinal microbiota (dysbiosis; Salzman and Bevins, 2013). Dysbiosis, however, exacerbates the underlying diseases, thus creating a vicious cycle between the host and microbiota.

Graft-versus-host disease (GVHD) is an alloreactive, donor T cell–mediated inflammatory disease that occurs after allogeneic hematopoietic stem cell transplantation (SCT), involving the skin, liver, and gastrointestinal tract (Ferrara et al., 2009). We and others have shown that GVHD leads to a loss of Paneth cells and mediates intestinal dysbiosis (Eriguchi et al., 2012; Jenq et al., 2012). The dysbiosis that occurs in MHC-mismatched mouse models of GVHD is remarkable and thus represents a feasible tool to test novel strategies to modulate dysbiosis (Eriguchi et al., 2012).

Current strategies to restore the gut ecosystem are bacteriotherapy, using diet, prebiotics/probiotics, and fecal microbiota transplantation; however, no physiological approach has been developed so far. Here, we demonstrate a novel approach to restore intestinal microbial ecology and prevent dysbiosis by Wnt agonist R-Spondin1 (R-Spo1; Kim et al., 2005; Takashima et al., 2011) or recombinant α-defensin (Tomisawa et al., 2015) in mice. The Wnt agonist R-Spo1, which binds to leucine-rich repeat–containing G protein–coupled receptor (Lgr) 5, is one of the essential factors to build intestinal villus-crypt units from a single $Lgr5^+$ intestinal stem cell (ISC; Sato et al., 2009; de Lau et al., 2011; Farin et al., 2016). We found that R-Spo1 stimulates ISCs to differentiate to Paneth cells and enhanced luminal secretion of α-defensins. In ad-

Correspondence to Takanori Teshima: teshima@med.hokudai.ac.jp; Daigo Hashimoto: D5hash@pop.med.hokudai.ac.jp

Abbreviations used: Ab, antibody; AMP, antimicrobial peptide; BM, bone marrow; CM, complete medium; EEC, enteroendocrine cell; EGFP, enhanced GFP; GVHD, graft-versus-host disease; ISC, intestinal stem cell; MMP-7, matrix metalloproteinase-7; PERMANOVA, permutational ANOVA; rRNA, ribosomal RNA; SCT, hematopoietic stem cell transplantation.



The Rockefeller University Press
J. Exp. Med. 2017 Vol. 214 No. 12 3507–3518
https://doi.org/10.1084/jem.20170418



The Journal of Experimental Medicine

dition, administration of R-Spo1 or the recombinant mouse α-defensin cryptdin-4 (Crp4) prevents GVHD-mediated dysbiosis after SCT. Such approaches represent a physiological approach at modifying the gut ecosystem to restore intestinal homeostasis and host–microbiota cross talk toward therapeutic benefits. Because dysbiosis has a role in the pathogenesis of many diseases, such approaches have broad potential in individuals at risk or with various diseases.

## RESULTS AND DISCUSSION

### R-Spo1 stimulates ISC differentiation to Paneth cells and enhances Paneth cell production of α-defensins

R-Spo1 enhances the proliferation of cycling ISCs via the Wnt/β-catenin signaling pathway and generates crypt-villus organoids from ISCs in vitro (Sato et al., 2009). We previously showed that administration of R-Spo1 stimulated proliferation of ISCs and induced crypt cell hyperplasia in vivo (Kim et al., 2005; Takashima et al., 2011). However, the effects of R-Spo1 on Paneth cell proliferation and function remain to be determined. Here, we first addressed whether R-Spo1 could increase the number of Paneth cells in vivo. R-Spo1 was i.v. injected to B6D2F1 mice at a dose of 200 μg for 6 d. The number of Paneth cells morphologically identified as cells containing eosinophilic granules in H&E staining was significantly increased in all sites of the small intestine, including duodenum, jejunum, and ileum of R-Spo1–treated mice (Fig. 1, A and B). R-Spo1 significantly elongated crypt depth (Fig. 1 C). Although Kim et al. (2005) showed that daily injection of R-Spo1 at a dose of 100 μg for 3 d did not increase Paneth cell numbers, differences in dose and duration of the R-Spo1 used may explain the discrepancy in the results between studies. Immunofluorescence studies demonstrated that Paneth cells generated by R-Spo1 coexpress lysozyme, Crp1, a subtype of α-defensins, and matrix metalloproteinase-7 (MMP-7), which converts pro–α-defensins into active form (Fig. 1, D and E). These results indicate that they are functionally mature Paneth cells (Wilson et al., 1999). Similar results were obtained in BALB/c mice, ruling out the strain-specific effects of R-Spo1 on Paneth cell expansion (Fig. S1, A–C). There were some MMP-7$^+$ Crp1$^-$ cells in R-Spo1–treated mice (Fig. 1 E and Fig. S1 C). Although characteristics of these cells remain to be elucidated, Wnt activation may lead to precocious differentiation of progenitors into Paneth cells (Tian et al., 2015).

R-Spo1 also increased the number of enhanced GFP (EGFP)$^+$ ISCs in B6-*Lgr5-EGFP-creER* mice, in which Lgr5$^+$ ISCs were marked, as we previously reported (Fig. S1, D and E; Takashima et al., 2011). All intestinal epithelial cells, including Paneth cells, are progenies of ISCs (Barker et al., 2007). We therefore addressed whether R-Spo1 stimulated ISCs to differentiate to de novo Paneth cells or expanded mature Paneth cells in fate-mapping reporter mice, in which Lgr5$^+$ ISCs and their progenies are visually identified as RFP$^+$ cells. Administration of R-Spo1 for 3 d increased RFP$^+$ Paneth cells, indicating that R-Spo1 stimulated differentiation of ISCs toward Paneth cells (Fig. 1, F and G).

We next addressed whether other intestinal cell types were also expanded by R-Spo1. Alcian blue staining of the small intestine demonstrated that R-Spo1 increased goblet cells, but the expansion of goblet cells occurred to a lesser extent compared with that of Paneth cells (Fig. 1, B and H). Immunofluorescence staining of chromogranin A showed R-Spo1 did not significantly increase enteroendocrine cells (EECs) in the small intestine (Fig. 1, I and J). The mechanisms by which R-Spo1 preferentially expands Paneth cells compared with other cell types in the small intestine remains to be elucidated. One possible explanation could be that Paneth cell differentiation is more strictly dependent on Wnt/β-catenin signaling than other cell types (Yin et al., 2014). Both Wnt activation and Notch suppression in ISCs promote ISCs to differentiate to Paneth cells (VanDussen et al., 2012; Tian et al., 2015). We next studied expression of delta-like (Dll) 1 and Dll4, canonical Notch ligands that suppress progenitor differentiation to Paneth cells. R-Spo1 significantly decreased the expression of *Dll4* in the small intestine, and there was a trend toward reduced expression of *Dll1* in R-Spo1–treated animals compared with controls ($P = 0.06$), suggesting that R-Spo1 activated Wnt signaling but suppressed Notch signaling (Fig. 1, K and L). Although the molecular mechanisms by which R-Spo1 suppresses Notch ligands remain to be elucidated, Wnt and Notch signaling in ISCs could be reciprocally controlled, as Notch inhibition enhances Wnt activation (Tian et al., 2015).

We then evaluated whether administration of R-Spo1 could lead to increased luminal secretion of α-defensins, the most potent AMP class from Paneth cells (Ayabe et al., 2000; Salzman et al., 2010). Fecal samples were collected after administration of R-Spo1. An ELISA (Nakamura et al., 2013) demonstrated that R-Spo1 significantly increased fecal levels of α-defensins Crp1 and Crp4 (Fig. 1, M and N; and Fig. S1, F and G). We addressed whether increased production of α-defensins could be caused by an increase in Paneth cell production on a per-cell basis. Quantitative PCR of Paneth cells purified from the isolated crypts showed expression levels of *Defa4* and *Mmp7* were not increased, indicating that increased production of α-defensins was merely a reflection of an increased number of Paneth cells by R-Spo1 (Fig. 1, O and P).

These data showed novel in vivo effects of R-Spo1: it promptly stimulates ISCs to differentiate to functionally maturated Paneth cells and increases intraluminal levels of α-defensins. We then addressed whether increased secretion of α-defensins into the lumen could alter the composition of intestinal microbiota of healthy naive mice using bacterial 16S ribosomal RNA (rRNA) sequences of the fecal pellets. Permutational analysis of variance (PERMANOVA) of the genus composition did not detect a significant alteration of intestinal microbial composition after R-Spo1 treatment ($P = 0.62$), although there was a minor alteration of some genera (Fig. S1 H). These data suggested that transient up-regulation of α-defensins has minimal bactericidal activity against certain commensals living together with a host in a symbiotic

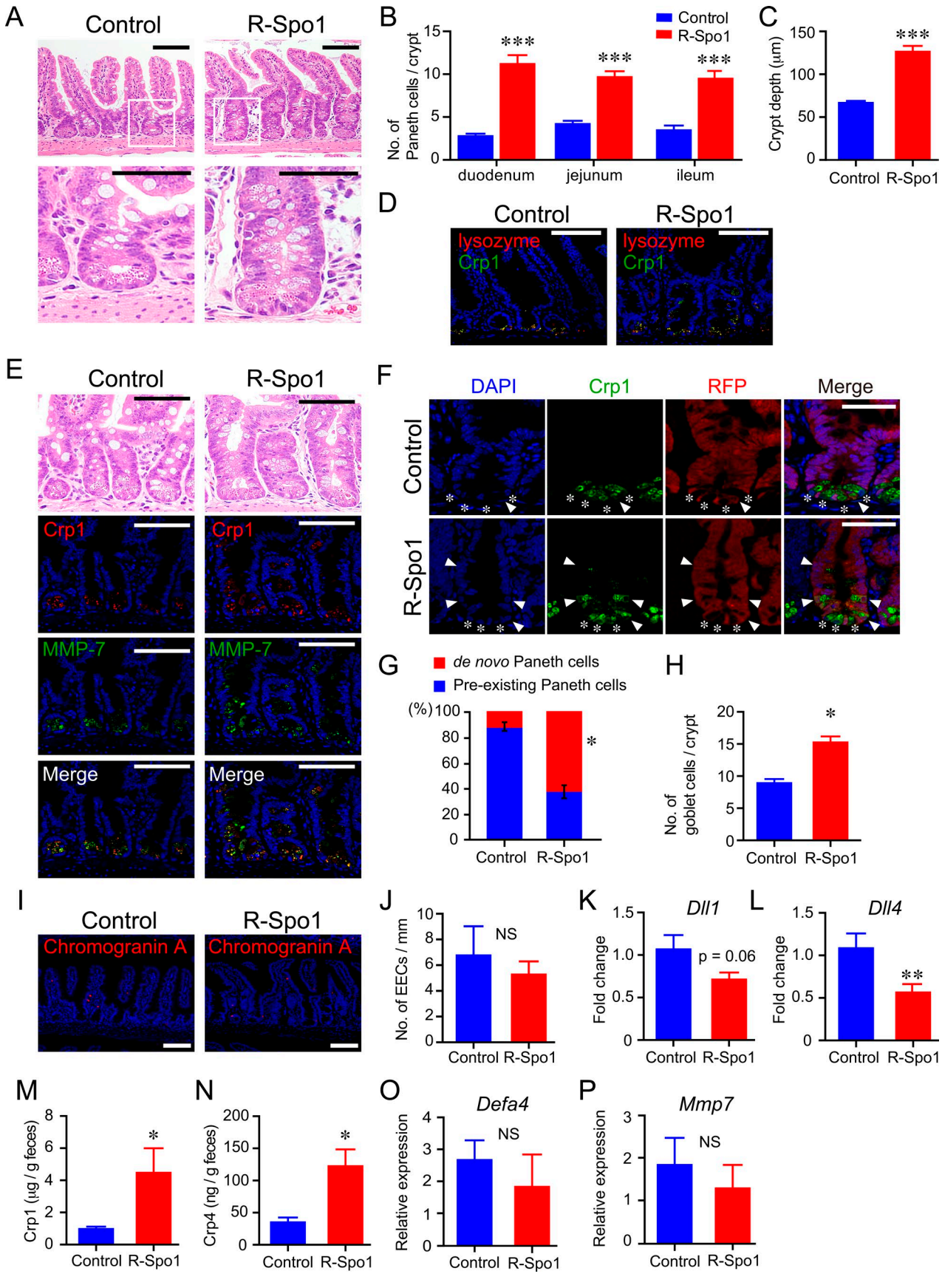
A
Control
R-Spo1
B
Control
R-Spo1
No. of Paneth cells / crypt
15
10
5
0
***
***
***
duodenum
jejunum
ileum
C
Crypt depth (μm)
150
100
50
0
***
Control
R-Spo1
D
Control
R-Spo1
lysozyme
Crp1
lysozyme
Crp1
E
Control
R-Spo1
Crp1
Crp1
MMP-7
MMP-7
Merge
Merge
F
DAPI
Crp1
RFP
Merge
Control
R-Spo1
G
de novo Paneth cells
Pre-existing Paneth cells
(%)100
80
60
40
20
0
*
Control
R-Spo1
H
No. of goblet cells / crypt
20
15
10
5
0
*
Control
R-Spo1
I
Control
R-Spo1
Chromogranin A
Chromogranin A
J
No. of EECs / mm
10
8
6
4
2
0
NS
Control
R-Spo1
K
Dll1
Fold change
1.5
1.0
0.5
0
p = 0.06
Control
R-Spo1
L
Dll4
Fold change
1.5
1.0
0.5
0
**
Control
R-Spo1
M
Crp1 (μg / g feces)
8
6
4
2
0
*
Control
R-Spo1
N
Crp4 (ng / g feces)
200
150
100
50
0
*
Control
R-Spo1
O
Defa4
Relative expression
4
3
2
1
0
NS
Control
R-Spo1
P
Mmp7
Relative expression
3
2
1
0
NS
Control
R-Spo1

relationship, as previously reported (Ouellette et al., 1994; Ayabe et al., 2000; Masuda et al., 2011). However, the effects of chronic administration of R-Spo1 on microbial composition remain to be elucidated because genetic overexpression of human defensin 5 in mice alters gut microbiota composition (Salzman et al., 2010).

### R-Spo1 protects Paneth cells from GVHD and prevents intestinal dysbiosis

Historically, an impact of the intestinal microbiota on disease development was first described in mouse models of GVHD using germ-free mice or gut-decontaminating antibiotics in the early 1970s (Jones et al., 1971). GVHD is an alloreactive donor T cell–mediated inflammatory disease involving the gut, skin, and liver after allogeneic SCT (Teshima et al., 2002). We and others have reported that GVHD mediates Paneth cell injury and subsequent intestinal dysbiosis in association with reduced levels of α-defensins (Eriguchi et al., 2012; Jenq et al., 2012, 2015; Levine et al., 2013; Holler et al., 2014). Because α-defensins have minimal bactericidal effects against certain commensal bacteria and predominantly target pathogenic bacteria, loss of α-defensins may be causally related to the reduction of commensal bacteria and the compensatory outgrowth of pathogenic bacteria. Alternately, AMP loss may alter the ecological interaction between bacterial species or host immune reaction against commensal bacteria or reduce bacterial niche for commensal bacteria (Faust and Raes, 2012). To evaluate dysbiosis associated with the loss of Paneth cells and the reduced secretion of α-defensin, lethally irradiated B6D2F1 or B6D2F1-*Lgr5-EGFP-creER* ($H\text{-}2^{b/d}$) mice were i.v. injected with $5 \times 10^6$ bone marrow (BM) cells + $5 \times 10^6$ splenocytes from MHC-mismatched B6 ($H\text{-}2^{b}$) donors on day 0. Immunofluorescence analysis of the small intestine on day 7 showed that α-defensin–expressing Paneth cells were severely reduced in allogeneic animals compared with syngeneic controls (Fig. 2, A–C; and Fig. S2 A). In parallel with Paneth cell loss, fecal levels of α-defensin Crp4 were significantly lower in allogeneic animals on day 7 than those in syngeneic controls (Fig. 2 D), although bacterial load in fecal pellets was not changed between syngeneic and allogeneic mice (Fig. 2 E). Bacterial 16S rRNA sequences of the fecal pellets showed significant dysbiosis 7 d after allogeneic SCT, whereas there was no alternation of bacterial composition in syngeneic controls compared with those in naive mice (Fig. 2 F and Fig. S2, B–D). A principal component analysis and PERMANOVA demonstrated a significant difference in the bacterial composition between allogeneic and syngeneic animals (Fig. 2, G and H). There were significant correlations between GVHD severity and the proportion of specific microbes on day 7 after allogeneic SCT. Abundances of Proteobacteria at the phylum level, Enterobacteriales at the order level, and *Escherichia* and *Bacteroides* at the genus level were negatively correlated with the body weight of mice, whereas those of the phylum Firmicutes, the order Clostridiales, and the genus *Lactobacillus* were positively correlated with the body weight of mice (Fig. 2, I–K; and Fig. S2, E–H). These data confirmed that GVHD-mediated reduction of AMPs resulted in the loss of symbiotic bacteria that have immunoregulatory or homeostatic roles in the intestine, as well as the expansion of pathogenic proinflammatory bacteria (Gerbitz et al., 2004; Heimesaat et al., 2010; Eriguchi et al., 2012; Jenq et al., 2012). We hypothesize that R-Spo1 could inhibit the expansion of pathogenic noncommensals with the protection of symbiotic beneficial bacteria by expanding Paneth cells and increasing α-defensins after SCT.

To test whether R-Spo1 could protect Paneth cells after SCT, recipient mice were i.v. injected with R-Spo1 at a dose of 100 µg from day −3 to −1 and day 1 to 3 after SCT, and Paneth cells were enumerated on day 7 and 28 after SCT. As expected, R-Spo1 protected Paneth cells against GVHD-mediated damages, and significantly more Paneth cells persisted on days 7 and 28 after SCT in R-Spo1–treated allogeneic recipients compared with allogeneic controls (Fig. 2, A–C; and Fig. S2 A). We also confirmed that R-Spo1 was protective against ISC damages (Fig. S3 A) and ameliorated GVHD pathology such as severe blunting of villi and inflammatory infiltration (Fig. 2 B). Furthermore, R-Spo1 treatment significantly restored fecal levels of mouse α-defensin Crp4 as high as the levels of syngeneic mice (Fig. 2 D). To evaluate whether R-Spo1 reduces intestinal

Figure 1. **R-Spo1 treatment promotes development of Paneth cells from ISCs and increases luminal concentrations of α-defensins.** (A–E and H–P) B6D2F1 mice were i.v. injected with R-Spo1 (200 µg/d) or PBS for 6 d. 1 d later, the small intestine was harvested. (A) H&E staining. Bars: (top) 100 µm; (bottom) 30 µm. Areas in the white squares are magnified and shown below the original images. (B) Numbers of Paneth cells per crypt ($n = 6$ per group). (C) Crypt depth ($n = 4$ per group). (D) Confocal images. Lysozyme and Crp1 are expressed by Paneth cells. Bar, 100 µm. (E) Serial sections of the small intestine. H&E staining (top), confocal images of Crp1, MMP-7, and the merged images of Crp1 and MMP-7. Bars, 100 µm. (F and G) *Lgr5-EGFP-creER*×*R26*$^{Tomato}$ mice were i.p. injected with 40 mg/kg tamoxifen for 3 d to label ISCs, followed by i.v. injection of R-Spo1 (200 µg/d) for 3 d. (F) Confocal images of lineage tracing in the small intestine are shown. RFP is expressed by $Lgr5^+$ ISCs and their progenies, and Crp1 is expressed by Paneth cells. Asterisks indicate preexisting Paneth cells. Arrowheads indicate de novo generated Paneth cells from $Lgr5^+$ ISCs. Bars, 50 µm. (G) Numbers of preexisting and de novo Paneth cells per crypt in the ileum ($n = 3$ per group). (H) Numbers of goblet cells per crypt ($n = 4$ per group). (I) Confocal images. Chromogranin A is expressed by EECs. Bars, 50 µm. (D–F and I) DAPI (blue) stains the nucleus. (J) Numbers of EECs per 1 mm of ileum ($n = 5$ per group). (K and L) Quantitative real-time PCR analysis of *Dll1* or *Dll4* transcripts in the small intestine normalized to those of 18S rRNA ($n = 10$ per group). (M and N) Fecal levels of Crp1 and Crp4. (O and P) mRNA extracted from highly purified Paneth cells was subjected to quantitative PCR analysis of Defa4 and Mmp7. Relative expression of mRNA in purified Paneth cells is shown by the comparative ΔCt method ($n = 3$ per group). (B, C, G, H, and J–P) Data from two independent experiments were combined and are shown as means ± SE. Student's *t* tests or Mann–Whitney *U* tests were used to compare the data. *, $P < 0.05$; **, $P < 0.01$; ***, $P < 0.001$.

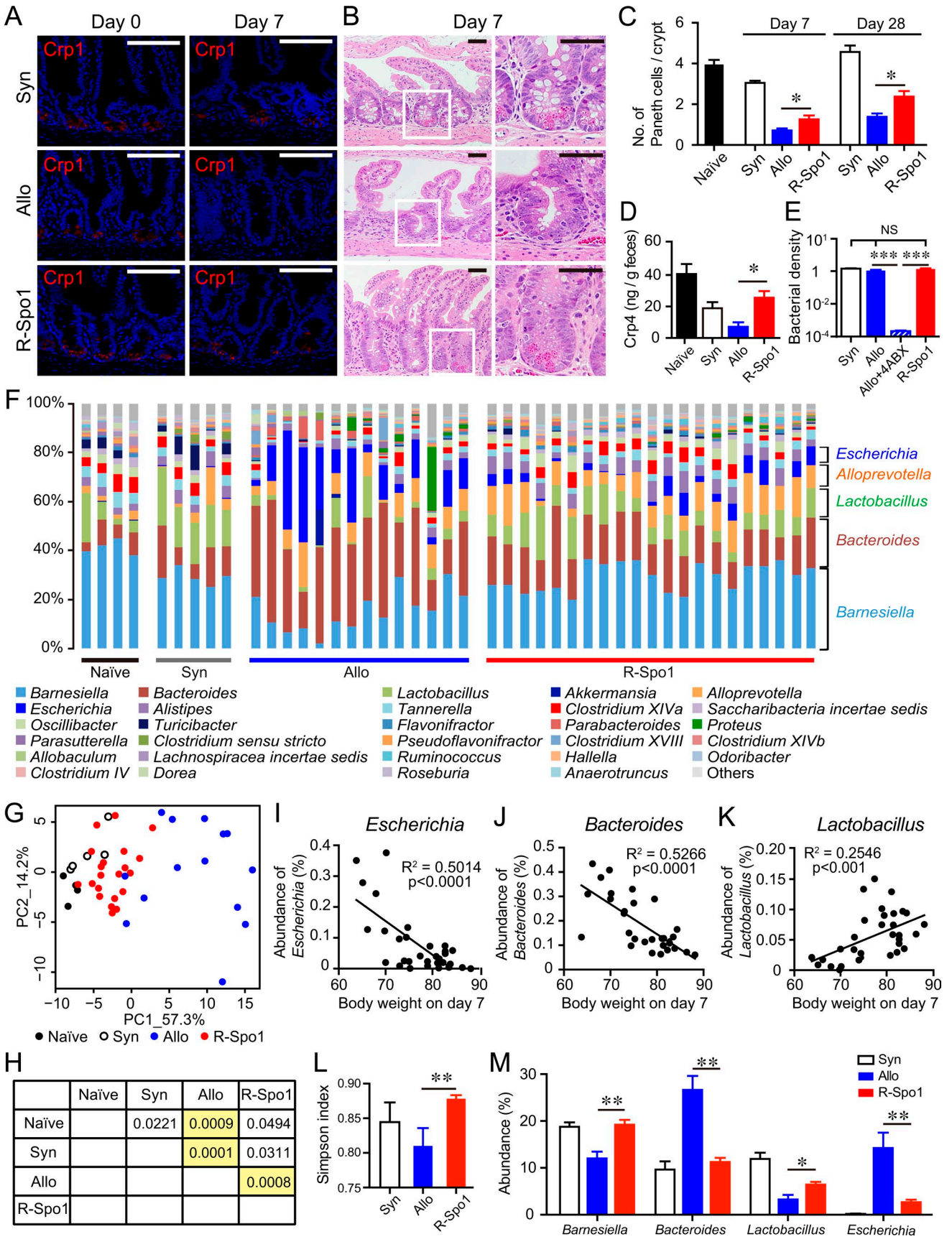


| | Naïve | Syn | Allo | R-Spo1 |
|---|---|---|---|---|
| Naïve | | 0.0221 | 0.0009 | 0.0494 |
| Syn | | | 0.0001 | 0.0311 |
| Allo | | | | 0.0008 |
| R-Spo1 | | | | |

Table 1. **Differences in specific bacteria at the genus levels after SCT between groups**

| Genus | Naive vs. Allo | Syn vs. Allo | Allo vs. R-Spo1 |
|---|---|---|---|
| *Barnesiella* | 0.0006536[a] | 0.01231[a] | 1.48E-05[a] |
| *Bacteroides* | 0.0006536[a] | 0.004294[a] | 0.0009352[a] |
| *Lactobacillus* | 0.1013 | 0.002161[a] | 0.000145[a] |
| *Alloprevotella* | 0.04641 | 0.1483 | 0.1446 |
| *Escherichia* | 0.0006536[a] | 0.003431[a] | 0.0003294[a] |
| *Alistipes* | 0.2771 | 0.00819 | 1.78E-06[a] |
| *Clostridium XIVa* | 0.001307[a] | 0.006634 | 0.0007021[a] |
| *Tannerella* | 0.0006536[a] | 0.00535 | 2.74E-05[a] |
| *Oscillibacter* | 0.002614[a] | 0.08408 | 0.0001718[a] |
| *Saccharibacteria genera incertae sedis* | 0.0006536[a] | 0.07217 | 5.89E-07[a] |
| *Proteus* | 0.03464[a] | 0.01443 | 0.04695 |
| *Parabacteroides* | 0.0006536[a] | 0.01499 | 2.74E-05[a] |

SCT was performed and R-Spo1 was administered as in Fig. 2. Naive, $n = 4$; Syn, $n = 5$; Allo, $n = 14$; R-Spo1, $n = 21$.
[a]$P < 0.005$.

bacterial load, fecal bacterial loads in R-Spo1–treated mice were measured with quantitative PCR targeting 16S rRNA and compared with those in the mice treated with a combination of four antibiotics, including ampicillin, streptomycin, vancomycin, and metronidazole from day −7 of transplantation. In sharp contrast with the dramatically reduced bacterial load in mice treated with antibiotics, R-Spo1 did not affect bacterial load (Fig. 2 E). 16S rRNA sequences of the fecal pellets showed that microbiome compositions of R-Spo1–treated mice significantly differed from those of allogeneic controls but were rather similar to that of syngeneic controls (Fig. 2, F–H; and Fig. S2, B–D). R-Spo1 restored intestinal microbiome diversity to the levels of that in syngeneic controls, as determined by a Simpson index (Fig. 2 L; Simpson, 1949). It also inhibited GVHD-associated outgrowth of *Escherichia* and *Bacteroides* and reduction of *Barnesiella* and *Lactobacillus* (Fig. 2 M and Table 1). Together with the data showing R-Spo1 had minimal effects on commensals in naive mice, these results represent in vivo confirmation of a selective bactericidal activity of α-defensins increased by R-Spo1 against noncommensal bacteria, which we and others have shown in vitro (Ouellette et al., 1994; Masuda et al., 2011). In association with prevention of dysbiosis, brief administration of R-Spo1 significantly suppressed donor T cell infiltration into the small intestine (Fig. S3 B). These data indicate that R-Spo1 prevents GVHD-associated dysbiosis and dampens allogeneic immune responses after allogeneic SCT.

### Oral administration of recombinant Crp4 partially prevents dysbiosis and GVHD

α-Defensins are the most potent AMPs, which account for 70% of the Paneth cell-derived AMP activity (Ayabe et al., 2000; Salzman et al., 2010). Finally, we addressed whether direct administration of α-defensin could modify the intestinal microbiota. We generated Crp4, the most bactericidal mouse α-defensin (Tomisawa et al., 2015). Crp4 was orally administered at a dose of 125 μg twice daily from day 3 to 7 after SCT and resulted in increased fecal levels of Crp4 measured by ELISA, which detects only conformationally native form, not changed or reduced form, indicating that Crp4 was not degenerated before reaching the intestines (Fig. 3 A; Nakamura et al., 2013). Administration of Crp4 significantly ameliorated GVHD-mediated dysbiosis (Fig. 3 B) and restored microbiome diversity (Fig. 3 C) without altering the bacterial load on day 7 (Fig. 3 D). There was a significant difference in the bacterial composition between Crp4-treated animals and allogeneic controls on day 7 (Fig. 3, E and F). Crp4 significantly inhibited the GVHD-associated outgrowth of *Bacteroides* at genus level (44.9 ± 4.5% vs. 28.0 ± 3.8%; $P = 0.038$), and there were trends of reduced Enterobacteriales (11.3 ± 3.2% vs. 3.78 ± 3.3%; $P = 0.11$) and increased Clostridiales (17.6 ± 3.0% vs. 32.6 ± 6.2%; $P = 0.067$) at order levels in Crp4-treated animals compared with allogeneic controls (Fig. 3, G and H). Oral administration of Crp4 also significantly suppressed donor T cell infiltration into the small intestine, liver, and spleen (Fig. S3, C–E) and significantly mitigated weight loss and clinical GVHD scores on day 21 after SCT (Fig. 3, I and J). The flora shift toward the widespread prevalence of *Bacteroides* and *Escherichia* in GVHD (Fig. 2 F and Fig. 3 B), as has been shown (Eriguchi et al., 2012), in-

Figure 2. **R-Spo1 protects Paneth cells from GVHD and prevents intestinal dysbiosis.** Lethally irradiated B6D2F1 mice were transplanted with BM cells plus splenocytes from B6 (Allo) or B6D2F1 (Syn) donors on day 0. Mice were treated with R-Spo1 or PBS on day −3 to −1 and day 1 to 3. (A) Confocal images of the small intestine on days 0 and 7. Crp1 with DAPI (blue) counterstaining. (B) H&E staining of the small intestine on day 7. Areas in the white squares are magnified and shown to the right of the original images. (C) Numbers of Paneth cells per crypt ($n = 4$–9 per group). (D) Fecal levels of Crp4 ($n = 4$–8 per group). (E) A group of mice received a combination of four antibiotics (4ABX) in drinking water from day −7. Ratio of bacterial load in fecal pellets on day 7 determined by quantitative PCR of 16S rRNA gene copies compared with that of naive mice ($n = 4$ per group). (F–M) Intestinal microbial compositions were determined by 16S rRNA sequencing (Naive, $n = 4$; Syn, $n = 5$; Allo, $n = 14$; R-Spo1, $n = 21$). (F) Each bar represents bacterial composition of an individual mouse at the genus level. (G) Principal component analysis of genus compositions of intestinal microbiota from each mouse. (H) The p-values of PERMANOVA of the genus compositions. Bonferroni-corrected statistically significant combinations are indicated in yellow. (I–K) Correlation analysis between body weight on day 7 after allogeneic SCT and abundance of the genus *Escherichia*, *Bacteroides*, and *Lactobacillus* determined by a linear regression using the Spearman analysis for nonparametric data. (L) Diversities of intestinal microbiome determined by a Simpson index at the genus level. (M) Abundances of specific bacteria at the genus levels. Data from two (C–E) or six (F–K) independent experiments were combined and are shown as means ± SE. (C–E, L, and M) Mann–Whitney *U* tests or one-way ANOVA followed by Tukey's posttest were used to compare the data. Bars, 50 μm. *, $P < 0.05$; **, $P < 0.01$; ***, $P < 0.001$.

creased the translocation of pathogen-associated molecular patterns, such as lipopolysaccharides into systemic circulation, and augmented donor T cell activation (Cooke et al., 2001). Crp4 suppressed the outgrowth of such pathogens (Fig. 3 B), as has been shown (Masuda et al., 2011), and thereby could suppress systemic donor T cell expansion. However, dysbiosis recurred after discontinuation of Crp4, and effects of Crp4 against GVHD were abrogated on day 35 (Fig. 3, B, C, E, F, I, and J). Although Crp4-treated mice showed a trend toward better survival early after SCT, the difference was eventually not significant (Fig. 3 K), suggesting that the brief administration of a single Crp subset may not be impactful enough to improve survival.

Although both R-Spo1 and Crp4 prevented dysbiosis, the effects of R-Spo1 were more potent than those of Crp4. We previously reported that short-term administration of R-Spo1 significantly prolonged survival after SCT, but the effects of short-term Crp4 on GVHD were modest. This is probably because R-Spo1 potentially increases AMPs from Paneth cells other than Crp4, such as Crp1 and lysozyme (Fig. 1, E, F, and N), and possibly other AMPs from other cells such as regenerating islet-derived protein 3 (Reg3) from enterocytes and exerts protective effects against ISCs and epithelial injury (Takashima et al., 2011).

Epithelial regeneration is critical for barrier maintenance for host defense and favorable immune responses (Takashima et al., 2011; Lindemans et al., 2015). α-Defensins lack protective effects on epithelium; intestinal epithelial injury impairs the beneficial effects of commensals on the host immune system (Nakahashi-Oda et al., 2016). IL-22 also promotes ISC-mediated intestinal epithelial regeneration (Lindemans et al., 2015); however, differentiation of ISCs toward Paneth cells requires Wnt/β-catenin signaling (Yin et al., 2014). Thus, R-Spo1 could more potently stimulate Paneth cell proliferation and secretion of α-defensins than IL-22. However, IL-22 increases enterocyte production of another AMP, Reg3 (Lindemans et al., 2015). A combined use of R-Spo1 and IL-22 may be an attractive strategy.

There is a cross talk between a host and microbiota. Normal microbiota is important for the host's health and a balanced immune system. Emerging data suggest that changes in the microbiota play a crucial role in the pathogenesis of both intestinal and nonintestinal disorders (Kamada et al., 2013; Mathewson et al., 2016; Teshima et al., 2016). The direct administration of a single AMP could be a novel approach to restore the gut ecosystem in dysbiosis. However, administration of R-Spo1 may modify the gut ecosystem more potently by increasing multiple AMPs from Paneth cells and possibly by other intestinal epithelial cells. Thus, the administration of R-Spo1 represents a novel physiological approach to restore the gut microbial ecosystem in order to ameliorate disease activity not only in GVHD, but also in various diseases in association with intestinal dysbiosis.

## MATERIALS AND METHODS

### Mice

Female C57BL/6 (B6: H-$2^b$, CD45.$2^+$), C57BL/6-Ly5a (B6-CD45.1: H-$2^b$, CD45.$1^+$), B6D2F1 (H-$2^{b/d}$, CD45.$2^+$), and DBA/2 (H-$2^d$, CD45.$2^+$) were purchased from CLEA Japan. Female BALB/c (H-$2^d$, CD45.$2^+$) mice were purchased from Charles River Japan. B6-*Lgr5-EGFP-creER* (*Lgr5-EGFP-IRES-creER*$^{T2}$) and B6-*R26*$^{Tomato}$ [*B6.Cg-Gt(ROSA)-26Sor*$^{tm14(CAG-tdTOMATO)Hze/J}$] mice were purchased from Jackson Laboratory. *Lgr5-EGFP-creER×R26*$^{Tomato}$ mice were generated by crossing B6-*R26*$^{Tomato}$ female mice with B6-*Lgr5-EGFP-creER* male mice. B6D2F1-*Lgr5-EGFP-creER* mice were generated by crossing B6-*Lgr5-EGFP-creER* male mice with DBA/2 female mice. All animal experiments were performed under the auspices of the Institutional Animal Care and Research Advisory Committee (approval number 12–0106). Experiments in this manuscript were performed in a nonblinded fashion. All mice for microbial analysis or the recipients of SCT were purchased from the same vendor and cohoused until they were used in the experiments.

### Reagents

Recombinant human R-Spo1 was generated as previously reported (Kim et al., 2005). Recombinant Crp4 was produced and purified as previously described (Tomisawa et al., 2015). Streptomycin and metronidazole purchased from Sigma-Aldrich and ampicillin and vancomycin purchased from Wako were given at a concentration of 1 mg/ml in drinking water.

### SCT

Mice were transplanted as previously described (Takashima et al., 2011). In brief, after lethal x-ray total body irradiation (11–13 Gy) delivered in two doses at 4-h intervals, mice were i.v. injected with $5 \times 10^6$ BM cells with $5 \times 10^6$ splenocytes. Female mice at 8–12 wk old were allocated randomly for each experimental group, ensuring the mean body weight in each group was similar. Mice were maintained in specific pathogen-free conditions and received normal chow and autoclaved acidic water, pH 2.5, after SCT. Survival after SCT was monitored daily, and the degree of clinical GVHD was assessed weekly by using a scoring system (Cooke et al., 1996). Sample size for survival experiments was aimed for 10 per group for 75% power to detect 60% difference in survival probabilities from the threshold with a one-sided type I error of 0.05.

### Histological and immunofluorescence analysis

For pathological analysis, samples of the small intestine were fixed in 4% paraformaldehyde, embedded in paraffin, sectioned, and stained with H&E or Alcian blue. Immunofluorescence analysis was performed using primary antibodies (Abs), including rabbit antilysozyme (A0099; Dako), rat anti-Crp1 (77-R63), rabbit anti–MMP-7 (D4H5; Cell Signaling Technology), chicken anti-EGFP (ab13970; Abcam), rabbit anti-RFP (ab34771; Abcam), and rabbit anti–chromogranin

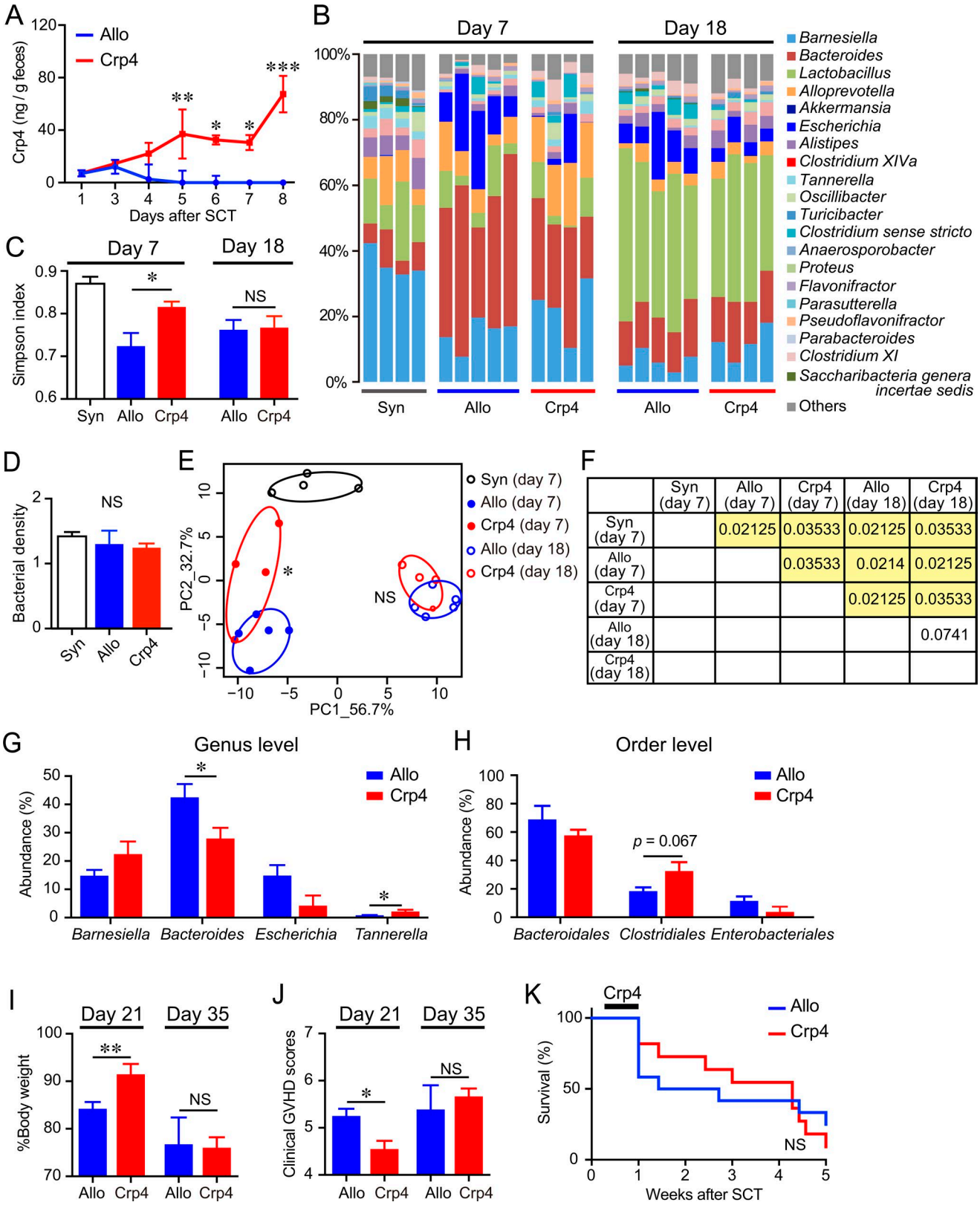


| | Syn (day 7) | Allo (day 7) | Crp4 (day 7) | Allo (day 18) | Crp4 (day 18) |
|---|---|---|---|---|---|
| Syn (day 7) | | 0.02125 | 0.03533 | 0.02125 | 0.03533 |
| Allo (day 7) | | | 0.03533 | 0.0214 | 0.02125 |
| Crp4 (day 7) | | | | 0.02125 | 0.03533 |
| Allo (day 18) | | | | | 0.0741 |
| Crp4 (day 18) | | | | | |

Figure 3. **Oral administration of Crp4 partially prevents dysbiosis and GVHD.** SCT was performed as in Fig. 2. Recipient mice were orally administered 125 µg Crp4 or control twice a day from day 3 to 7 after allogeneic SCT. (A) Fecal levels of Crp4 were measured with ELISA (means ± SE, $n = 6$ per group). (B, C, and E–H) Bacterial compositions of intestinal microbiota at the genus level determined by 16S rRNA sequencing on days 7 and 18 (B), Simpson di-

A (ab85554; Abcam), and visualized with Alexa Fluor 488–, 555–, and 647–conjugated secondary Abs. Pictures of tissue sections were taken at room temperature using a digital camera (DP20; Olympus) mounted on a microscope (BX50; Olympus), fluorescence microscope (BZ-X700; Keyence), and confocal laser microscope (FV-1000D; Olympus).

### Fate mapping of Lgr5$^+$ ISCs

*Lgr5-EGFP-creER×R26$^{Tomato}$* mice were i.p. injected with 40 mg/kg tamoxifen (Sigma-Aldrich) daily for 3 d to label ISCs, followed by i.v. injection of R-Spo1 of PBS daily for 3 d.

### Flow cytometric analysis

Monoclonal Abs conjugated with fluorescein isothiocyanate, phycoerythrin, phycoerythrin-Cy7, peridinin–chlorophyll protein complexes, allophycocyanin, and allophycocyanin-Cy7 were purchased from BD PharMingen, eBioscience, and Biolegend. In flow cytometric analysis, at least 300,000 live samples were analyzed using FACSCantoII (BD Biosciences) and FlowJo software (Tree Star).

### Lamina propria lymphocyte dissociation

The small intestine was isolated and opened with scissors along intestinal length. Samples were then incubated on a shaker in complete medium (CM; 2% FCS in PBS) in the presence of 1 mM DL-dithiothreitol (Sigma-Aldrich) at 37°C for 20 min and subsequently incubated with 1.3 mM EDTA (Nippon Gene) in CM at 37°C for 40 min. They were rinsed twice in CM and digested with 0.3 mg/ml of type IV collagenase (Sigma-Aldrich) at 37°C for 45 min, homogenized, filtered, and washed.

### ELISA

Fecal samples were prepared as previously described (Nakamura et al., 2013; Eriguchi et al., 2015). In brief, samples were air dried, powdered using a bead beater–type homogenizer (Beads Crusher μT-12; TAITEC). Fecal extract was collected after blending with PBS using a vortex mixer for 1 h at 4°C and centrifugation at 20,000 *g* for 20 min, and levels of Crp1 and Crp4 were measured by sandwich ELISA as previously described (Nakamura et al., 2013; Eriguchi et al., 2015).

### Preparation of crypt cells from the small intestine

For crypt isolation, mouse small intestine was flushed with cold PBS and cut open lengthwise in 10-cm-long pieces. The villi were scraped off using a scalpel blade, and remaining tissues were washed with cold PBS. After incubation with 30 mM EDTA in HBSS for 10 min at room temperature, the tissue fragments were shaken vigorously in fresh HBSS to exfoliate crypts. The dissociated crypts were further digested with shaking at 180 rpm in HBSS supplemented with 200 U/ml collagenase (Sigma-Aldrich), 10 μM Y-27632 (Sigma-Aldrich), and 1 mM *N*-acetylcysteine (Sigma-Aldrich) for 5 min at 37°C on a horizontal shaker (TAITEC). Crypt cells were then briefly treated with 50 μg/μl DNase I (Roche), filtered with a 40-μm cell strainer (BD Falcon), and subjected to Paneth cell purification.

### Paneth cell purification

Crypt cells were incubated with 10 μM Zinpyr-1 (Santa Cruz Biotechnology) for 10 min at 37°C to stain secretory granules in Paneth cells and filtered with Cell Strainer Snap Cap with 35-μm nylon mesh (BD Falcon). Zinpyr-1$^+$SSC$^{low}$ cells were sorted as Paneth cell–rich fraction using a cell sorter (JSAN; Bay Bioscience), and then Paneth cells identified as Zynpyr-1$^+$ granular cells using a confocal microscope (A1; Nikon) were aspirated one by one using a 50-μm glass micropipette (1-GT50S-5; Nepa Gene) with micromanipulators (MN-4 and MMO-202ND; Narishige) and an electronic pipette (PicoPipet; Nepa Gene).

### Reverse transcription

50 Paneth cells were lysed in 4 μl lysis buffer of SingleShot cell lysis kit (Bio-Rad Laboratories) and subjected to reverse transcription using an iScript Advanced cDNA synthesis kit for quantitative real-time PCR (Bio-Rad Laboratories) and a thermal cycler (Veriti; Thermo Fisher Scientific). For preparation of cDNA from the small intestine, total RNA from frozen tissues was extracted using ISOGEN II (Nippon Gene). cDNA was synthesized using ReverTra Ace qPCR RT Master Mix with gDNA Remover (FSQ-301; Toyobo).

### Quantitative real-time PCR analysis

Quantitative real-time PCR was performed on the ABI StepOnePlus system using TaqMan Fast Advanced Master Mix and the primers and fluorescent TaqMan probe sets specific for mouse *Defa4* (Mm00651736_g1), *Mmp7* (Mm00487724_m1), *Dll1* (Mm01279269_m1), and *Dll4* (Mm00444619_m1; all from Applied Biosystems). The reactions were performed in a 96-well plate in triplicate. The 18S rRNA primer probe set was 5′-GCTCTTTCTCGATTC CGTGGG-3′ for the forward primer, 5′-ATGCCAGAG

versity index of intestinal microbiota on days 7 and 18 (C), principal component analysis of genus compositions of intestinal microbiota on day 7 (E), the q-values (false discovery rates) of PERMANOVA of genus compositions between groups (F), and abundances of specific bacteria at the genus levels (G) and order levels (H) are shown. Yellow highlighting in F indicates statistically significant values. (D) Ratio of bacterial load in fecal pellets on day 7 by quantitative PCR of 16S rRNA gene copies compared with that of naive mice (means ± SE, $n = 4$ per group). (I–K) Body weight (I) and clinical GVHD scores (J) on days 21 and 35 and survival curves (K) after SCT ($n = 12$ per group) are shown. (C–J) Data from one of two independent experiments with similar results are shown. (K) Data from two independent experiments were combined and are shown as means ± SE. (C, D, and G–J) Student's *t* tests or Mann–Whitney *U* tests were used to compare the data. (K) Log-rank test was used to compare survival curves. *, $P < 0.05$; **, $P < 0.01$; ***, $P < 0.001$.

TCTCGTTCGTTATC-3′ for the reverse primer, and FAM-CTCCACCAACTAAGAACGGCCATGCACC-TAMRA for the probe (Sigma-Aldrich), and the set was separately amplified in the same plate as an internal control for variation in the amount of cDNA in PCR.

### Quantification of fecal bacterial load

Fecal bacterial load was measured as previously described (Liang et al., 2015).

### 16S rRNA gene amplification and sequencing

Fresh fecal pellets were collected from each mouse. Total DNA was extracted using a PowerFecal DNA isolation kit (MO BIO Laboratories). The V3–V4 variable region of the 16S rRNA gene was amplified from fecal DNA extracts using the 16S metagenomic sequencing library protocol provided by Illumina. Samples were sequenced on the MiSeq sequencing platform according to standard Illumina sequencing protocols. Sequenced read data were deposited to the DNA Databank of Japan Sequence Read Archive with DRA accession nos. DRA005119 and DRA005031.

### Bioinformatics analysis

We discarded the reads that (a) contained ambiguous nucleotides and (b) were mapped to the PhiX genome sequence by a Bowtie 2 (version 2.2.3) search with default parameters (Langmead and Salzberg, 2012). Each forward and reverse read for the paired-end library was then merged by a USEARCH (version 7.0.1090) with a –fastq_truncqual 7 parameter (Edgar, 2010). Both the forward and reverse primer sequences were removed by a TagCleaner search with four mismatches allowed (Schmieder et al., 2010). We obtained the high-quality reads after removal of the reads that (a) contained <350 or >650 nt and (b) were associated with a mean Phred-like quality score of <25 as calculated by the Illumina MiSeq sequencer. Sequence clustering of the high-quality reads was conducted by using the UCLUST (version 7.0.1090) with identity >97% (Edgar, 2010) and query and reference coverage >80%. Chimeric operational taxonomic units were detected and removed if the operational taxonomic units were assigned to the chimera in both of the following two methods: (1) a UCHIME (version 7.0.1090) reference mode search against the reference gold database (http://drive5.com/uchime/gold.fa) and (2) a UCHIME de novo mode search (Edgar et al., 2011). Taxonomic assignment of the high-quality reads was performed by an RDP MultiClassifier (version 1.1) search with a bootstrap value >0.5 (Wang et al., 2007). Compositional differences of genera among mice with different treatments were visualized by a principal component analysis and statistically analyzed by a PERMANOVA with Bray–Curtis dissimilarity index in the vegan library of the R software. For multiple testing corrections, a false discover rate estimation was used in Fig. 3 F, whereas more conservative multiple testing corrections with Bonferroni correction was performed to reduce type I errors with the larger sample sizes in Fig. 2 H. Diversity of the microbial community was calculated using the Simpson's index with genus level (Simpson, 1949).

### Statistical analysis

Data were checked for normal distribution and similar variance between groups. Student's *t* tests were used to compare data between two groups when the data follow a normal distribution. Mann–Whitney *U* tests were used to compare data between two groups when the data did not follow a normal distribution. The Kaplan–Meier product limit method was used to obtain survival probability, and the log-rank test was applied to compare survival curves. Analyses were performed using JMP Pro (version 11.0.0; SAS) and Prism (version 7.0; GraphPad Software). $P < 0.05$ was considered statistically significant.

### Online supplemental material

Fig. S1 shows that R-Spo1 increases $Lgr5^+$ ISCs and Paneth cells in vivo. Fig. S2 that shows R-Spo1 protects Paneth cells against GVHD and ameliorates intestinal dysbiosis. Fig. S3 shows effects of R-Spo1 on ISCs, Paneth cells, and donor T cells and effects of Crp4 on donor T cells after SCT.

## ACKNOWLEDGMENTS

This study was supported by grants from the Ministry of Education, Culture, Sports, Science and Technology/Japan Society for the Promotion of Science KAKENHI (25293217 and 221S0002 to T. Teshima, 26461438 to D. Hashimoto, 26462831 to K. Nakamura, and 26440072 to T. Aizawa), Health and Labor Science Research grants from the Ministry of Health, Labour and Welfare (to T. Teshima), the Promotion and Standardization of the Tenure-Track System (to D. Hashimoto), the Astellas Foundation for Research on Metabolic Disorders (to D. Hashimoto), the Takeda Science Foundation (to D. Hashimoto), SENSHIN Medical Research Foundation (to D. Hashimoto), Global Station for Soft Matter, a project of the Global Institution for Collaborative Research and Education at Hokkaido University (to T. Aizawa), and the Center of Innovation Program from the Japan Science and Technology Agency (to T. Teshima, K. Nakamura, and T. Ayabe.).

The authors declare competing financial interests: T. Teshima is a recipient of a research grant from Kyowa Hakko Kirin.

Author contributions: E. Hayase, D. Hashimoto, and T. Teshima developed the conceptual framework of the study, designed the experiments, conducted studies, analyzed data, and wrote the paper. C. Noizat, R. Ogasawara, S. Takahashi, H. Ohigashi, Y. Yokoi, R. Sugimoto, K. Ebata, T. Yamakawa, S. Matsuoka, E. Yokoyama, T. Ara, and K. Nakamura conducted experiments. Y. Ogura, T. Hayashi, H. Mori, and K. Kurokawa conducted 16S rRNA gene sequencing and data analysis. K. Tomizuka produced R-Spo1. R. Hiramine and T. Aizawa produced Crp4. T. Kondo and T. Ayabe supervised experiments.

**Submitted: 5 March 2017**
**Revised: 9 July 2017**
**Accepted: 7 September 2017**

## REFERENCES

Ayabe, T., D.P. Satchell, C.L. Wilson, W.C. Parks, M.E. Selsted, and A.J. Ouellette. 2000. Secretion of microbicidal alpha-defensins by intestinal Paneth cells in response to bacteria. *Nat. Immunol.* 1:113–118. https://doi.org/10.1038/77783

Barker, N., J.H. van Es, J. Kuipers, P. Kujala, M. van den Born, M. Cozijnsen, A. Haegebarth, J. Korving, H. Begthel, P.J. Peters, and H. Clevers. 2007.

Identification of stem cells in small intestine and colon by marker gene Lgr5. *Nature.* 449:1003–1007. https://doi.org/10.1038/nature06196

Cooke, K.R., L. Kobzik, T.R. Martin, J. Brewer, J. Delmonte Jr., J.M. Crawford, and J.L. Ferrara. 1996. An experimental model of idiopathic pneumonia syndrome after bone marrow transplantation: I. The roles of minor H antigens and endotoxin. *Blood.* 88:3230–3239.

Cooke, K.R., A. Gerbitz, J.M. Crawford, T. Teshima, G.R. Hill, A. Tesolin, D.P. Rossignol, and J.L. Ferrara. 2001. LPS antagonism reduces graft-versus-host disease and preserves graft-versus-leukemia activity after experimental bone marrow transplantation. *J. Clin. Invest.* 107:1581–1589. https://doi.org/10.1172/JCI12156

de Lau, W., N. Barker, T.Y. Low, B.K. Koo, V.S. Li, H. Teunissen, P. Kujala, A. Haegebarth, P.J. Peters, M. van de Wetering, et al. 2011. Lgr5 homologues associate with Wnt receptors and mediate R-spondin signalling. *Nature.* 476:293–297. https://doi.org/10.1038/nature10337

Edgar, R.C. 2010. Search and clustering orders of magnitude faster than BLAST. *Bioinformatics.* 26:2460–2461. https://doi.org/10.1093/bioinformatics/btq461

Edgar, R.C., B.J. Haas, J.C. Clemente, C. Quince, and R. Knight. 2011. UCHIME improves sensitivity and speed of chimera detection. *Bioinformatics.* 27:2194–2200. https://doi.org/10.1093/bioinformatics/btr381

Eriguchi, Y., S. Takashima, H. Oka, S. Shimoji, K. Nakamura, H. Uryu, S. Shimoda, H. Iwasaki, N. Shimono, T. Ayabe, et al. 2012. Graft-versus-host disease disrupts intestinal microbial ecology by inhibiting Paneth cell production of α-defensins. *Blood.* 120:223–231. https://doi.org/10.1182/blood-2011-12-401166

Eriguchi, Y., K. Nakamura, D. Hashimoto, S. Shimoda, N. Shimono, K. Akashi, T. Ayabe, and T. Teshima. 2015. Decreased secretion of Paneth cell α-defensins in graft-versus-host disease. *Transpl. Infect. Dis.* 17:702–706. https://doi.org/10.1111/tid.12423

Farin, H.F., I. Jordens, M.H. Mosa, O. Basak, J. Korving, D.V. Tauriello, K. de Punder, S. Angers, P.J. Peters, M.M. Maurice, and H. Clevers. 2016. Visualization of a short-range Wnt gradient in the intestinal stem-cell niche. *Nature.* 530:340–343. https://doi.org/10.1038/nature16937

Faust, K., and J. Raes. 2012. Microbial interactions: from networks to models. *Nat. Rev. Microbiol.* 10:538–550. https://doi.org/10.1038/nrmicro2832

Ferrara, J.L., J.E. Levine, P. Reddy, and E. Holler. 2009. Graft-versus-host disease. *Lancet.* 373:1550–1561. https://doi.org/10.1016/S0140-6736(09)60237-3

Gerbitz, A., M. Schultz, A. Wilke, H.J. Linde, J. Schölmerich, R. Andreesen, and E. Holler. 2004. Probiotic effects on experimental graft-versus-host disease: let them eat yogurt. *Blood.* 103:4365–4367. https://doi.org/10.1182/blood-2003-11-3769

Heimesaat, M.M., A. Nogai, S. Bereswill, R. Plickert, A. Fischer, C. Loddenkemper, U. Steinhoff, S. Tchaptchet, E. Thiel, M.A. Freudenberg, et al. 2010. MyD88/TLR9 mediated immunopathology and gut microbiota dynamics in a novel murine model of intestinal graft-versus-host disease. *Gut.* 59:1079–1087. https://doi.org/10.1136/gut.2009.197434

Holler, E., P. Butzhammer, K. Schmid, C. Hundsrucker, J. Koestler, K. Peter, W. Zhu, D. Sporrer, T. Hehlgans, M. Kreutz, et al. 2014. Metagenomic analysis of the stool microbiome in patients receiving allogeneic stem cell transplantation: loss of diversity is associated with use of systemic antibiotics and more pronounced in gastrointestinal graft-versus-host disease. *Biol. Blood Marrow Transplant.* 20:640–645. https://doi.org/10.1016/j.bbmt.2014.01.030

Jenq, R.R., C. Ubeda, Y. Taur, C.C. Menezes, R. Khanin, J.A. Dudakov, C. Liu, M.L. West, N.V. Singer, M.J. Equinda, et al. 2012. Regulation of intestinal inflammation by microbiota following allogeneic bone marrow transplantation. *J. Exp. Med.* 209:903–911. https://doi.org/10.1084/jem.20112408

Jenq, R.R., Y. Taur, S.M. Devlin, D.M. Ponce, J.D. Goldberg, K.F. Ahr, E.R. Littmann, L. Ling, A.C. Gobourne, L.C. Miller, et al. 2015. Intestinal Blautia Is Associated with Reduced Death from Graft-versus-Host Disease. *Biol. Blood Marrow Transplant.* 21:1373–1383. https://doi.org/10.1016/j.bbmt.2015.04.016

Jones, J.M., R. Wilson, and P.M. Bealmear. 1971. Mortality and gross pathology of secondary disease in germfree mouse radiation chimeras. *Radiat. Res.* 45:577–588. https://doi.org/10.2307/3573066

Kamada, N., S.U. Seo, G.Y. Chen, and G. Núñez. 2013. Role of the gut microbiota in immunity and inflammatory disease. *Nat. Rev. Immunol.* 13:321–335. https://doi.org/10.1038/nri3430

Kim, K.A., M. Kakitani, J. Zhao, T. Oshima, T. Tang, M. Binnerts, Y. Liu, B. Boyle, E. Park, P. Emtage, et al. 2005. Mitogenic influence of human R-spondin1 on the intestinal epithelium. *Science.* 309:1256–1259. https://doi.org/10.1126/science.1112521

Langmead, B., and S.L. Salzberg. 2012. Fast gapped-read alignment with Bowtie 2. *Nat. Methods.* 9:357–359. https://doi.org/10.1038/nmeth.1923

Levine, J.E., E. Huber, S.T. Hammer, A.C. Harris, J.K. Greenson, T.M. Braun, J.L. Ferrara, and E. Holler. 2013. Low Paneth cell numbers at onset of gastrointestinal GVHD identify patients at high risk for nonrelapse mortality. *Blood.* 122:1505–1509. https://doi.org/10.1182/blood-2013-02-485813

Liang, X., F.D. Bushman, and G.A. FitzGerald. 2015. Rhythmicity of the intestinal microbiota is regulated by gender and the host circadian clock. *Proc. Natl. Acad. Sci. USA.* 112:10479–10484. https://doi.org/10.1073/pnas.1501305112

Lindemans, C.A., M. Calafiore, A.M. Mertelsmann, M.H. O'Connor, J.A. Dudakov, R.R. Jenq, E. Velardi, L.F. Young, O.M. Smith, G. Lawrence, et al. 2015. Interleukin-22 promotes intestinal-stem-cell-mediated epithelial regeneration. *Nature.* 528:560–564. https://doi.org/10.1038/nature16460

Masuda, K., N. Sakai, K. Nakamura, S. Yoshioka, and T. Ayabe. 2011. Bactericidal activity of mouse α-defensin cryptdin-4 predominantly affects noncommensal bacteria. *J. Innate Immun.* 3:315–326. https://doi.org/10.1159/000322037

Mathewson, N.D., R. Jenq, A.V. Mathew, M. Koenigsknecht, A. Hanash, T. Toubai, K. Oravecz-Wilson, S.R. Wu, Y. Sun, C. Rossi, et al. 2016. Gut microbiome-derived metabolites modulate intestinal epithelial cell damage and mitigate graft-versus-host disease. *Nat. Immunol.* 17:505–513. https://doi.org/10.1038/ni.3400

Nakahashi-Oda, C., K.G. Udayanga, Y. Nakamura, Y. Nakazawa, N. Totsuka, H. Miki, S. Iino, S. Tahara-Hanaoka, S. Honda, K. Shibuya, and A. Shibuya. 2016. Apoptotic epithelial cells control the abundance of Treg cells at barrier surfaces. *Nat. Immunol.* 17:441–450. https://doi.org/10.1038/ni.3345

Nakamura, K., N. Sakuragi, and T. Ayabe. 2013. A monoclonal antibody-based sandwich enzyme-linked immunosorbent assay for detection of secreted α-defensin. *Anal. Biochem.* 443:124–131. https://doi.org/10.1016/j.ab.2013.08.021

Ouellette, A.J., M.M. Hsieh, M.T. Nosek, D.F. Cano-Gauci, K.M. Huttner, R.N. Buick, and M.E. Selsted. 1994. Mouse Paneth cell defensins: primary structures and antibacterial activities of numerous cryptdin isoforms. *Infect. Immun.* 62:5040–5047.

Qin, J., R. Li, J. Raes, M. Arumugam, K.S. Burgdorf, C. Manichanh, T. Nielsen, N. Pons, F. Levenez, T. Yamada, et al. MetaHIT Consortium. 2010. A human gut microbial gene catalogue established by metagenomic sequencing. *Nature.* 464:59–65. https://doi.org/10.1038/nature08821

Salzman, N.H., and C.L. Bevins. 2013. Dysbiosis--a consequence of Paneth cell dysfunction. *Semin. Immunol.* 25:334–341. https://doi.org/10.1016/j.smim.2013.09.006

Salzman, N.H., K. Hung, D. Haribhai, H. Chu, J. Karlsson-Sjöberg, E. Amir, P. Teggatz, M. Barman, M. Hayward, D. Eastwood, et al. 2010. Enteric defensins are essential regulators of intestinal microbial ecology. *Nat. Immunol.* 11:76–82. https://doi.org/10.1038/ni.1825

Sato, T., R.G. Vries, H.J. Snippert, M. van de Wetering, N. Barker, D.E. Stange, J.H. van Es, A. Abo, P. Kujala, P.J. Peters, and H. Clevers. 2009. Single Lgr5 stem cells build crypt-villus structures in vitro without a mesenchymal niche. *Nature.* 459:262–265. https://doi.org/10.1038/nature07935

Schmieder, R., Y.W. Lim, F. Rohwer, and R. Edwards. 2010. TagCleaner: Identification and removal of tag sequences from genomic and metagenomic datasets. *BMC Bioinformatics.* 11:341. https://doi.org/10.1186/1471-2105-11-341

Simpson, E.H. 1949. Measurement of diversity. *Nature.* 163:688. https://doi.org/10.1038/163688a0

Takashima, S., M. Kadowaki, K. Aoyama, M. Koyama, T. Oshima, K. Tomizuka, K. Akashi, and T. Teshima. 2011. The Wnt agonist R-spondin1 regulates systemic graft-versus-host disease by protecting intestinal stem cells. *J. Exp. Med.* 208:285–294. https://doi.org/10.1084/jem.20101559

Teshima, T., R. Ordemann, P. Reddy, S. Gagin, C. Liu, K.R. Cooke, and J.L. Ferrara. 2002. Acute graft-versus-host disease does not require alloantigen expression on host epithelium. *Nat. Med.* 8:575–581. https://doi.org/10.1038/nm0602-575

Teshima, T., P. Reddy, and R. Zeiser. 2016. Acute Graft-versus-Host Disease: Novel Biological Insights. *Biol. Blood Marrow Transplant.* 22:11–16. https://doi.org/10.1016/j.bbmt.2015.10.001

Tian, H., B. Biehs, C. Chiu, C.W. Siebel, Y. Wu, M. Costa, F.J. de Sauvage, and O.D. Klein. 2015. Opposing activities of Notch and Wnt signaling regulate intestinal stem cells and gut homeostasis. *Cell Reports.* 11:33–42. https://doi.org/10.1016/j.celrep.2015.03.007

Tomisawa, S., Y. Sato, M. Kamiya, Y. Kumaki, T. Kikukawa, K. Kawano, M. Demura, K. Nakamura, T. Ayabe, and T. Aizawa. 2015. Efficient production of a correctly folded mouse α-defensin, cryptdin-4, by refolding during inclusion body solubilization. *Protein Expr. Purif.* 112:21–28. https://doi.org/10.1016/j.pep.2015.04.007

VanDussen, K.L., A.J. Carulli, T.M. Keeley, S.R. Patel, B.J. Puthoff, S.T. Magness, I.T. Tran, I. Maillard, C. Siebel, Å. Kolterud, et al. 2012. Notch signaling modulates proliferation and differentiation of intestinal crypt base columnar stem cells. *Development.* 139:488–497. https://doi.org/10.1242/dev.070763

Wang, Q., G.M. Garrity, J.M. Tiedje, and J.R. Cole. 2007. Naive Bayesian classifier for rapid assignment of rRNA sequences into the new bacterial taxonomy. *Appl. Environ. Microbiol.* 73:5261–5267. https://doi.org/10.1128/AEM.00062-07

Wilson, C.L., A.J. Ouellette, D.P. Satchell, T. Ayabe, Y.S. López-Boado, J.L. Stratman, S.J. Hultgren, L.M. Matrisian, and W.C. Parks. 1999. Regulation of intestinal alpha-defensin activation by the metalloproteinase matrilysin in innate host defense. *Science.* 286:113–117. https://doi.org/10.1126/science.286.5437.113

Yin, X., H.F. Farin, J.H. van Es, H. Clevers, R. Langer, and J.M. Karp. 2014. Niche-independent high-purity cultures of Lgr5+ intestinal stem cells and their progeny. *Nat. Methods.* 11:106–112. https://doi.org/10.1038/nmeth.2737